Deep hypothermia prevents striatal alterations produced by perinatal asphyxia: implications for the prevention of dyskinesia and psychosis.

Short title: Deep hypothermia prevents striatal alterations produced by perinatal asphyxia.

Vázquez-Borsetti Pablo[1]., Andrés Acuña[1], Manuel Soliño[1], Juan José López-Costa[1], Lucila Kargieman[2], Fabián César Loidl[1].

1)Laboratorio de Neuropatología Experimental. Instituto de Biología Celular y Neurociencia “Prof. E. De Robertis”. UBA-CONICET. 2) IFIBYNE (UBA - CONICET) Instituto de Fisiología, Biología Molecular y Neurociencias - Universidad de Buenos Aires.

Correspondence to pvazquez@conicet.gov.ar.

Acknowledgement: We thank Francisco Urbano for his helpful insight and Luciana D'Alessio for her help with NeuN and calbindin immunohistochemistry. This research was supported by grants from the Consejo Nacional de Investigaciones Científicas y Técnicas (CONICET).

The data that support the findings of this study are available from the corresponding author upon reasonable request.

The authors declare non-financial competing interests or other conflicts of interests for this article.

This article has been accepted for publication and undergone full peer review but has not been through the copyediting, typesetting, pagination and proofreading process which may lead to differences between this version and the Version of Record. Please cite this article as doi: 10.1002/cne.24925

.

Abstract: The main neuronal population of the striatum are GABAergic medium spiny neurons. Calbindin is preferentially expressed in medium spiny neurons involved in the indirect pathway.

The aim of the present work is to analyze the effect of perinatal asphyxia on different subpopulations of GABAergic neurons in the striatum and to assess the outcome of deep therapeutic hypothermia.

The uterus of pregnant rats were removed by caesarean section and the fetuses were exposed to hypoxia by immersion in water (19 min) at 37 C° (perinatal asphyxia). The hypothermic group was exposed to 10 C° during 30 min after perinatal asphyxia. The rats were euthanized at the age of one month (adolescent/adult rats), their brains were dissected out and coronal sections were immunolabeled for calbindin, Calretinin, NeuN, and reelin. Reelin+ cells showed no staining in the striatum besides subventricular zone. The perinatal asphyxia (PA) group showed a significant decrease in calbindin neurons and a paradoxical increase in neurons estimated by NeuN staining. Moreover, Calretinin+ cells, a specific subpopulation of GABAergic neurons, showed an increase caused by perinatal asphyxia. Deep hypothermia reversed most of these alterations probably by protecting calbindin neurons. Similarly, there was a reduction of the diameter of the anterior commissure produced by the asphyxia that was prevented by hypothermic treatment.

Keywords: hypothermia, psychosis, perinatal asphyxia, RRID: AB_1603148, RRID: AB_563448, RRID: AB_2298772, RRID: AB_10846469, RRID: AB_228305, RRID: AB_2633275.

1 Introduction

Well established consequences of perinatal asphyxia (PA) include: Attention Deficit Hyperactivity Disorder, epilepsy, mental retardation and cerebral palsy or spasticity which manifest in the short and long term (Foster-Barber et al., 2001; Shankaran et al., 1991). Among these sequelae, there are two groups of symptoms that appear to be interconnected; an increased vulnerability to schizophrenia (Zornberg et al., 2000) and motor deficits including involuntary movements such as athetosic chorea (Plum, 1965).

The schizophrenia spectrum is characterized by psychosis that involves deliriums/hallucinations, social isolation and flat affect. Neuronal changes in schizophrenia include a decrease in GABAergic subpopulations including calbindin containing neurons among others (Reynolds et al., 2004).

The striatum is a key structure in the pathophysiology of schizophrenia as well as in the pathophysiology of dyskinesia. This structure has high density of calbindin+ neurons and it also represents one of the major pools of D2 receptor expression in the brain (Hurd et al., 2001). This is important, not only because D2 antagonism is the therapeutic target of antipsychotics, but because this compounds are also used in the treatment of chorea/dyskinesia (reviewed by (Coppen & Roos, 2017)). There

are also reports of cross-vulnerabilities for both pathologies (Kindler et al., 2016; Koning et al., 2011; Whitty et al., 2009)

The dorsal striatum is thought to be involved mostly in motor behaviors, while ventral striatum (or nucleus accumbens, NAcc) is crucial for motivational, cognitive and emotional processes (Groenewegen, 2003; Robbins & Everitt, 1996).

Medium spiny neurons (MSN) are the large majority of striatal neurons, 95% in rodents. MSN are GABAergic neurons that can be separated into two subpopulations: the neurons of the direct pathway that mainly express dopamine D1 receptor and project to the internal globus pallidus, and the MSN of the indirect pathway that mostly express the dopamine D2 receptor and project to the lateral globus pallidus.

In addition to the projections to the globus pallidus, MSNs from the striatal matrix also project to the substantia nigra reticulata, whereas MSNs of the striosome project directly to dopaminergic nuclei such as substantia nigra compacta and ventral tegmental area (Gerfen et al., 1990; Gerfen & Scott Young, 1988; Watabe-Uchida et al., 2012); for a review see (Gerfen & Surmeier, 2011).

Nowadays the only available therapeutic approach to prevent the damage caused by PA is deep hypothermia. These therapies involve mild hypothermia over long periods of time and have proven to be effective in mitigating the damage caused by PA in animal models and in humans. Some procedures involve exposition to a cooled blanket until rectal temperature reaches 33.5 ° C for 72 hours. Significant

improvements on survival and severe disabling sequelae have been reported under these conditions (Meloni et al., 2008; Simbruner et al., 2010).

In previous works from our group, deep hypothermia prevented histological alterations in medial prefrontal cortex and anterior insular cortex. PA decreased the density of calbindin+ neurons in the anterior insular cortex and deep hypothermia reversed this alteration. There were also behavioral alterations involving social interaction such as a decrease in play soliciting that also was reversed by deep hypothermia (Vázquez-Borsetti et al., 2018).

In order to deepen the knowledge about the mechanisms that generates dyskinesia and vulnerability to schizophrenia and to assess the therapeutic effect of hypothermia, we performed a set of immunohistochemical studies. We compared the densities of calbindin+, calretinin+ and NeuN+ cells among rats exposed to PA and PA+ therapeutic hypothermia. Calbindin is a good marker of MSN and it is distributed in the matrix of the striatum where the neurons preferentially participate in the indirect pathway (Bennett & Bolam, 1993). Calretinin is a marker of a specific subpopulation of GABAergic interneurons in the striatum (Petryszyn et al., 2018). Finally, the neuronal nuclear protein (NeuN) is a widely used neuronal marker (Azevedo et al., 2009) and we combined it with DAPI that stains all cell nuclei.

2 Methods

PA was induced in Sprague-Dawley albino rats using a noninvasive hypoxia-ischemia model, as described before (Loidl et al., 1994) . Housing and in vivo experiments were performed in the animal facility of the Facultad de Medicina de la Universidad de Buenos Aires. Personnel of the animal house controlled the welfare of the animals daily. The sick animals were euthanized or treated according to each case.

The animals were bred and handled in accordance with the guidelines published in the Guide for the Care and Use of Laboratory Animals CICUAL, and the principles presented in the "Guidelines for the Use of Animals in Neuroscience Research" by the Society for Neuroscience. The animal model described below was approved by the CICUAL ethics committee (Institutional Committee for the Care and Use of Laboratory Animals) (Resolution No. 2079/07), Faculty of Medicine, University of Buenos Aires, Argentina. Proper procedures were carried out to minimize the number of animals used, their suffering, pain and discomfort. This manuscript also complies with the ARRIVE (Animal Research: Reporting of In Vivo Experiments) guidelines. The rat animal model was selected because several aspects of the perinatal development are similar to human perinatal development. Rats also have more numerous litters and a very short life cycle making this species ideal for our experiments. The rationale for the selection of the present animal model is explained in the discussion. Animals were maintained at 24° C, with light / dark cycles over 12/12 hour, and provided with food and water ad libitum.

2.1 Treatment

Naive pregnant rats were euthanized by decapitation and were immediately hysterectomized after their first vaginal delivery. Term fetuses still in the womb were subjected to transient asphyxia by immersion of both uterine horns in a water bath for 19 minutes (18'30'' to 19'30'') at 37 ° C (PA and hypothermic group). After asphyxia, or immediately after hysterectomy in case of caesarean control (CC), the uterine horns were opened, pups were removed and stimulated to breathe. The pups were then placed for recovery under a heat lamp for an hour and were given to a surrogate mother. In the case of the group with hypothermia post asphyxia (HYPPA), pups were exposed to a temperature of 10 C ° for 30 min. At the end of the hypothermic shock, rectal temperature was measured with a thermocouple obtaining a temperature of 15 ± 1 °C. To avoid the influence of hormonal changes, only male rats were included in this study. The pups were weaned on postnatal day 25; litters were divided by sex and, males from the same mother were housed together. Sham rats were also included as controls, vaginal control (VC).

2.2 Histology and immunohistochemistry

In order to obtain the tissues for the immunohistochemical studies, either 3 or 4 rats 40 days old were selected within each experimental group (VC, CC and HYPPA, n=3 while PA, n=4). They were intraperitoneally anesthetized with an ip overdose of ketamine (250 mg/k) and xylazine 25 (mg/k) and perfused transcardially with 50 ml of saline solution, followed by 300 ml of fixative (4% paraformaldehyde) at room temperature. Brains were removed and stored for a period of time no longer than 2 days in phosphate buffered saline (PBS; pH 7.4; 4 °). Tissue sections of 40 µm of thickness were cut with a vibratome and stored in a

cryoprotective solution at -20 ° C. The sections were collected from rostral to caudal in multiwells. The firsts 10 sections from the beginning of the dorsal striatum were discarded and 3 wells per rat were filled sequentially with 15 slices each, starting around anteroposterior (AP) coordinate = 2.16 and ending on around AP= 0.36 (Paxinos & Watson, 2004). The start of the stria terminalis was used as landmark to stop collecting tissue (Figure 1). One section from each well (3 sections per rat) were preincubated for 30 min in 0.1 M PBS; 0.3% Triton X-100 and 1% goat serum at room temperature. Incubation with the primary antibody (1: 1000; mouse monoclonal, anti-reelin

(Abcam), anti-calbindin (Leica) or anti-NeuN (Millipore) was performed during 3-4 days at 4 ° C in multiwells (see table 1 for more information about the antibodies). Subsequently, sections were incubated for 120 minutes with biotinylated secondary antibody anti mouse (1: 1000, Thermo Fisher Scientific) followed by 30 min in Vectastain Elite ABC solution (Vector Laboratories). Sections were immersed in a solution of 0.05 mg / ml 3,3'-diaminobenzidine of containing 2 µl/ml of H_2O_2 and nickel ammonium until color development (in all cases less than 10 minutes). The reaction was stopped by performing two rinses in distilled H_2O.

In the case of fluorescent stain, the sections were incubated with an anti-mouse secondary antibody conjugated with Alexa 488 (Thermofisher Scientific, 1:1000). The stained sections were mounted on gelatin-coated slides for microscopic analysis.

2.3 Image analysis and cell counting.

In order to improve consistency of the data and decrease the impact of possible methodological errors, immunohistochemical studies were performed at least 3 times including different animals of all groups by each assay, with final N= 3-4. Because there was some variability among assays, we decided to normalize the results to the VC group counts that were considered as 100%. Systematic random sampling was used to obtain unbiased estimates of cell densities. Equidistant counting frames were generated and randomly assigned inside the region of interest using the grid tool from the program ImageJ (FIJI distribution).

The dimensions of the counting frames were determined with the aim of counting more than 150 cells per region of interest (ROI) in each slice. The sizes of the counting frames were 40 x 40 µm for calbindin and 30 x30 µm for DAPI and NEUN. The distances between frames were 280 µm for calbindin and 300 µm for DAPI and NEUN in the case of the dorsal striatum, and 40 µm and 30 µm, respectively, in the case of the nucleus accumbens.

The exception to this rule was the calretinin staining, due to the low number of cells we counted all cells inside the ROI. Manual counting was performed by a skilled counter blind to treatment using also ImageJ. All the cells inside the frame and in contact with 2 consecutive borders of the square were counted (but not the cells in contact with the other 2 borders). Within each experimental subject, 3 sections at different antero-posterior levels were analyzed. For DAPI, NeuN and Calbindin several images with X10 magnification were assembled in a panoramic picture covering the dorsal striatum sampling area (Figure 1, red square). In the case of

the calretinin immunostaining, the same analysis was performed but the panoramic composition was carried out with pictures of X20 magnification. Cell densities were calculated by dividing the number of cells counted by the sampled area. In the case of the nucleus accumbens, the anterior commissure was used as landmark to determine the region of interest. Also the start of the stria terminalis was used as landmark for the end of the structure. The delimitation of this ROI was determined in each case following Paxinos atlas as reference (Paxinos & Watson, 2004), an example can be seen in Figure 1 (yellow line). In all cases the focal point was settled outside of a guard zone of 2 µm from the surface. The thickness of the slice analyzed was 8.5 µm.

Results were reported using one-way ANOVA and the multiple comparison test of Holm-Sidak for post-hoc comparison. In all cases, the errors reported were standard errors. No outliers were excluded. The Shapiro-Wilk test indicated no significant deviation from normality and the Brown-Forsythe test indicated homogeneity of variances. For more information about unbiased counting see (Guillery, 2002) (Schmitz & Hof, 2005).

3 Results

3.1 Hypothermia prevents the decrease of calbindin neurons produced by PA in the dorsal and ventral striatum.

Immunostaining of calbindin neurons in the striatum showed a moderate stain compared to strong stained cells in the cortex. The distribution was uniform and there was high density of cells labeled except for some patches with low density

compatible with striosomes (Dorsal striatum Cell density in 0.01 mm^2 =21,27± 1,6, NAcc Cell density in 0.01 mm^2 = 15,49± 2,2). Striatum staining also showed slightly higher background than the cortex. The top of the dorsal striatum showed lower staining and was thus excluded of the sampling area. There was a significant decrease in the relative density of calbindin neurons in the PA group both in the dorsal striatum (-63,32% ±8,2; F (2, 7) = 41,04 P = 0,0001; PA vs. CC P = 0,0002; HYPPA vs. PA P = 0,0002) and in the NAcc (-69,90% ±16,9; F (2, 7) = 12,47 P = 0,0049; CC vs. PA P = 0,0087 HYPPA vs. PA P = 0,0071). In all cases, deep hypothermia reversed the alterations produced by asphyxia (Figure 2).

These changes do not seem to be accompanied by changes in the gross morphology of the striate. We measured the width of the structure and it did not show differences between control and PA groups (unpaired t test P = 0.16) (figure 1). See tables 2 and 5 for more information about statistical testing.

3.2 PA increases the number of neurons with calretinin in the dorsal striatum and deep hypothermia prevents this alteration.

In order to analyze if there is a compensatory increase of other subtypes of GABAergic neurons we performed reelin and calretinin immunohistochemical studies. Reelin labeling did not show any positive staining in the striatum apart from the subventricular zone where there was a group of cells with very strong labeling (Figure 3).

Calretinin neurons showed strong staining with low density of neurons scattered in the structure. The cell densities in the control group were 0,40± 0,06 . cells / 0.01

mm^2 in the dorsal striatum and 0,44 ± 0,11cells /.0.01 mm^2 in the ventral striatum. The relationship of calbindin/calretinin cells in the area was greater than 50 to 1(Figure 3).

In the dorsal striatum there was a significant increase of neurons with calretinin produced by asphyxia (126,6% ±25,12) and deep hypothermia prevented this alteration (F (2, 6) = 13,52 P = 0,006; HYPPA vs. PA P = 0,021CC vs. PA P = 0,0047). In the case of NAcc, a similar pattern was observed but with no significant differences (F (2, 6) = 0,69 P = 0,53) (Figure 3). See table 2 for more information about statistical testing.

3.3 NeuN immunohistochemistry and a DAPI stain.

After the aforementioned observations and with the objective of understanding how these alterations affect other neurons and cells in the structure, we performed a NeuN immunohistochemistry and a DAPI staining.

PA produced a significant increase (36,09% ± 10,56) in the number of total neurons of the dorsal striatum estimated by NeuN staining (F (2, 6) = 5,87 P =0,038; HYPPA vs. PA P = 0,342 CC vs. PA P= 0,028).

DAPI staining in the dorsal striatum generated a similar pattern although the differences did not reach statistical significance (F (2, 6) = 4,04 P = 0,077)

In the NAcc the same pattern was reproduced. A significant difference (F (2, 6) = 10,89 P = 0,01) was obtained in the ANOVA with a significant increase in NeuN

density in the PA group (48,66 % ± 11,12). This increase was prevented by the hypothermic treatment (HYPPA vs. PA P = 0,011). As in the case of dorsal striatum, the nuclear stain (DAPI) followed the same pattern than NeuN, although in this case the differences were less evident and did not reach significant differences either (F (2, 6) = 0,87P = 0,46) (Figure 3). The cell densities of the VC group were 26,24 ±1,65 cells in 0.01 mm^2 for NeuN and 46,35 ±5,07cells in 0.01 mm^2 for DAPI in the dorsal striatum. In the case of the ventral striatum, the density was 21,22 ±1,97 in 0.01 mm^2 for NeuN and 50,89 ±3,67 in 0.01 mm^2 for DAPI (Figure 4 and 5). See table 3 for more information about statistical testing.

3.4 Morphometric analysis of the anterior commissure

In order to analyze the health of the white matter a morphometric analysis of the anterior commissure was performed. The comparison of the nuclei density between groups did not show a significant difference (F (2, 6) = 0,58 P = 0,582). We also measured the thickness of the structure in the minor axis, a notorious shrinkage of the anterior commissure was produced by PA, (-30.36% ±8.39) this was reversed by deep hypothermia (F (2, 6) = 11.05 P = 0.009 HYPPA vs. PA P = 0.009 CC vs. PA P = 0.01). The VC values for these parameters were 0.325 ± 0.01 mm in the case of the minor axis of the anterior commissure and 63,83 ± 1,58 for DAPI cell counts (Figure 6). See table 4 for more information about statistical testing.

4 Discussion:

In the present work we found that perinatal asphyxia induced significant morphological and histological alterations in the rat striatum. These alterations were prevented by exposure to deep hypothermia.

4.1 **Calbindin:** The decrease in neurons with calbindin produced by asphyxia is noteworthy. This phenomenon was widely observed previously by our group and elsewhere. Decrease of calbindin+ neurons has been reported in the striatum (George et al., 2007; Guan et al., 1999; Mallard et al., 1995; W. D J Van De Berg et al., 2003) in the Prefrontal Cortex (Vázquez-Borsetti et al., 2016) and in the Anterior Insular Cortex (Vázquez-Borsetti et al., 2018) among others. Calbindin expressing neurons of the striatum correspond to a subpopulation of MSN, although there is also a small subpopulation that appear to be interneurons that do not have spines (Bennett & Bolam, 1993; Celio, 1990; DiFiglia et al., 1989; Prensa et al., 1998; Tripathi et al., 2010). Calbindin+ cells are preferentially distributed in the matrix where there is a majority of neurons that also co-express the D2 dopamine receptor and participate mostly in the indirect pathway (see (Brimblecombe & Cragg, 2017).

We also found a relatively high proportion of neurons with calbindin compared to total neurons, estimated by NeuN. These results are not surprising if we take into

consideration that 95 % of the striatal neurons correspond to medium-sized spiny neurons (Kemp & Powell, 1971).

The specific vulnerability of calbindin+ GABAergic neurons could be related, among others, to the excitatory-to-Inhibitory GABA switch that occurs at birth. During this period, It has been reported that interneurons are both; the source and the target of the first synapses, and glutamatergic transmission is mostly silent (Hennou et al., 2002). This excitatory GABAergic transmission generate giant depolarizing potentials (Ben-Ari, 2014). This phenomenon was observed in rodents and primates but there is evidence supporting similar process in humans. For example, GABAergic agonists generate epileptiform spasms at birth in rodents, primates and humans (Khazipov et al., 2001). Also, the use of GABAergic agonists in human newborns is highly contraindicated because they generate strong adverse and paradoxical effects (Chess & D'Angio, 1998; Ng et al., 2002).

4.2 Hypothermia:

An important characteristic of the therapeutic strategy used in this work is the period of exposition to hypothermia that is needed to accomplish its therapeutic effect. There is a relationship between the time of exposition and the final temperature needed to generate the therapeutic effect.

This treatment avoided the decrease in calbindin neuronal density caused by PA. Currently, the only therapeutic strategy available to treat perinatal asphyxia involves mild hypothermia, approximately 33º for 72 hours (Simbruner et al., 2010).

We believe that it is possible to reduce the time of exposure to hypothermia by using lower temperatures. Moreover, we think that lower temperatures as the ones used in this work could produce a stronger therapeutic effect. In previous studies with the same conditions, we saw that the exposure to a hypothermic shock of 15 C ° for 30 min prevented the death of interneurons in cortex (Vázquez-Borsetti et al., 2018). In this work we observed the same therapeutic effect in the striatum. An interesting fact is that another group tested an intermediate step with hypothermia of 30 °C during 90 min, obtaining similar results in the sheep. This group also used as an indicator of damage the decrease of calbindin cells in the striatum (George et al., 2007).

Input from deep hypothermia during aortic arch surgery indicates that the great majority of adults and children can be supported unharmed under a circulatory arrest by 30 minutes at 18 ° C (Fleck et al., 2003; Parissis et al., 2011).

The mechanism involved in the protective effect of hypothermia is more complex than a simple reduction in metabolism. Hypothermia is especially good to protect from excitotoxic damage (Leaw et al., 2017). Probably the mechanisms include: 1) Reduction of neuronal firing. 2) Restoration of the resting membrane potential (Thompson et al., 1985). 3) Reduction of metabolism during the reuptake of the intracellular calcium. 4) Reuptake of neurotransmitters from the synaptic cleft.

In a previous work we reported that hypothermia during asphyxia does not prevent the deterioration in social interaction produced by PA, but it was therapeutic when administered after asphyxia (Vázquez-Borsetti et al., 2018). Although, it is well

known that hypothermia during asphyxia has a strong protective effect (Loidl et al., 1998), this injury is characterized by two phases of damage. One phase takes place during asphyxia and the other takes place during reperfusion. It appears that social interaction is more vulnerable to reperfusion injury. The three main factors linked to this damage are: excitotoxic damage, inflammation and oxidative damage by reactive oxygen species.

Hypothermia generates a decrease in available oxygen that can be beneficial in the case of oxidative damage. In this sense, it is important not to generate a forced rewarming, but rather to allow the body to recover slowly the temperature (Scaravilli et al., 2012; Wong, 1983). Finally, hypothermia is also very well known for having anti-inflammatory properties (Zhao et al., 2019).

4.3 Increase in calretinin, NeuN and DAPI

Perinatal asphyxia increases the density of neurons with calretinin in the striatum. Although this result seems paradoxical, it has already been reported by other group (Yang et al., 2008). We hypothesize that this increase is caused by a compensatory effect exerted by the loss of calbindin neurons. The fact that deep hypothermia also prevents this alteration supports this interpretation.

The neurons with calretinin in the striatum are interneurons (Petryszyn et al., 2018) then, a priori, they could not correct the damage in the indirect pathway.

PA produced a slight but significant increase in NeuN density. Cell density estimated by DAPI staining followed the same pattern without reaching significant statistical differences. Other important piece of information is that the morphometry did not show any contraction/shrinkage of the structure. Human and rat brains continue to grow after birth (Anon, 1984; Fish & Winick, 1969; Ortinau et al., 2018). The loss of calbindin cells leaves space that could be occupied by other neurons. If the cell body and neuropil of the new neurons use less space than the former neurons, an increase in cell density seems plausible.

Another factor that may be contributing to this result is a homeostatic increase in other cell types to maintain the inhibitory balance of the structure. In previous studies we have found similar results in the anterior insular cortex with reelin-calretinin neurons. The increase in calretinin observed in this work is not enough to explain the compensation/increase in NeuN. Then, we predict increased cell density of other neuronal subpopulations in the striatum. If some of these neurons belong to the direct pathway, the imbalance between the direct and indirect pathway would be even greater than expected. This could reduce even further the inhibitory capacity of the striatum and increase the effect of dopamine in the structure worsening the symptoms of dyskinesia and psychosis. This point of view, is supported by previous works where PA produced an increase in the number of cells labeled using antibodies against neuronal nitric oxide synthase and cyclic guanosine monophosphate in the striatum (Barkhuizen, Van de Berg, et al., 2017). This is consistent with previous related research in the same model of asphyxia, where an increased striatal cGMP production was found at P10 (Loidl et al., 1998).

The nitric oxide synthase immunoreactive neurons where reported to express dopamine D1 receptor (and/or D5) and partially co-localize with parvalbumin neurons. The cGMP+ neurons match the MSN subpopulation (Arcangeli et al., 2013; Ariano, 1983)

Additionally, an interesting finding was the presence of reelin+ cells in the subventricular zone but not in the rest of striatum.

As far as we know, this is the first time that the presence of reelin in the subventricular zone has been reported, a fact that may have important implications for the role of reelin during neuronal development in one of the few cerebral areas that maintains neuronal proliferation during adulthood.

We did not find evidence of reelin+ cells in the adult striatum in this work with the exception of the subventricular zone. Some groups have reported that reelin labeling decreases during early postnatal development up to undetectable levels at PND14 (Alcántara et al., 1998) (Nishikawa et al., 1999). However other groups reported the presence of reelin in the adult mouse striatum (Arlotta et al., 2008; Cocas et al., 2009; Sharaf et al., 2015). It seems possible that the differences arise from discrepancies in the criteria to avoid false positive staining. It would be important to address this problem using more sensitive techniques.

Anyhow, it is interesting that the only place in the striatum where neurogenesis is maintained in adulthood is the subventricular zone where a clear and strong reelin labeling persists.

4.4 Anterior commissure.

White matter deterioration caused by perinatal asphyxia has been described elsewhere (Barkhuizen, van den Hove, et al., 2017; Bonestroo et al., 2015). A recent work showed a decrease in the thickness of the anterior commissure produced by PA in rabbits (Drobyshevsky, 2017). In this work we confirm this observation in rats and show that deep hypothermia reverses this alteration. This result may also have implications in schizophrenia since it has been reported the presence of white matter changes in schizophrenic patients (Bakhshi & Chance, 2015) including alterations in the anterior commissure (Choi et al., 2011). Inside the AC there were no variations in nucleus density (mostly belonging to glial cells). The stain does not differentiate among oligodendrocytes and astrocytes.

4.5 Limitations and methodological considerations:

Rat development has several differences with humans. Among these, a major concern of some colleagues stems from the differences in the peak of speed in growth rate. With the intention of "solving" this problem, a few models were proposed where the asphyxia is produced in postnatal day 7. These models do not take into consideration a large number of factors that are specific of birth, such as the excitatory / inhibitory switch of GABAergic neurons, among many others. We do not support the use of rats to PND7 for the study of perinatal asphyxia. We have already addressed this issue with more detail in previous works (see the discussion of (Vázquez-Borsetti et al., 2018).

In Figure 1 we show the relationship between different neuronal populations of the striatum, the proportions of the figure are a representation of the proportions estimated by cell counts. Anyhow, it is better to take it as an approximation because the data comes from three different techniques, DAPI immunohistochemistry with DAB and immunofluorescence.

Calretinin increase does not show significant differences in the nucleus accumbens, this is probably due to the combination of a low cell density with a small sampling area. This generates high error margins, but it is very probable the NAcc follows the same pattern as the dorsal striatum.

Of course, there could be alternative explanations for the reduction of calbindin+ neurons. PA could produce a disruption in the cellular expression of calbindin cells without killing them. If that were the case, we would observe an apparent decrease of neurons with calbindin, but the spiny neurons of the indirect pathway would be preserved. We find such explanation unlikely for many reasons. First, it is well known that PA kills cells and the mechanisms involved were widely described already (Northington et al., 2011), whereas the mechanism underlying the disruption of calbindin expression is not clear. Second, PA should decrease the expression of calbindin and also increase the expression of calretinin. However, those are two different cell populations. There is evidence suggesting that calretinin neurons share lineage with cholinergic neurons and not with MSN in the striatum (Garas et al., 2018). Last, the increase in NeuN does not support the hypothesis of a phenotype change in calbindin neither. If this was the case, the number of neurons should be kept constant. To further confirm the death of

calbindin neurons, future works will include double labeling with TUNEL staining, a widely accepted method for detecting apoptosis. It is worth to mention that an increase in TUNEL staining caused by PA in the striatum was already described (Wilma D.J. Van De Berg et al., 2002) . Taking into account the above considerations, our hypothesis is that the decrease of calbindin+ neurons generates indirectly the increase of other neuronal subtypes in an early stage of development.

4.6 Schizophrenia and dyskinesia:

The striatum plays an important role in the physiopathology of schizophrenia and many authors consider that it is related to the symptomatic dimension involved in psychosis (Morrison & Murray, 2009). Therefore, looking for strategies to avoid the damage of these neurons could prevent this psychiatric disease in patients who suffered PA. The similarities between PA and schizophrenia include symptomatic and pathophysiological aspects of the disease. 1) It has been seen in animal models that PA resembles positive symptoms and increases motor sensitivity to amphetamines. 2) PA produces deterioration in social interaction. 3) PA affects specific populations of GABAergic neurons without decreasing the total number of neurons. 4) PA produces a contraction of the prefrontal cortex and the anterior commissure. 5) PA decreases the number of synaptic spines in the prefrontal cortex (Herrera et al., 2017).

On the other hand, it is known that MSN damage is involved in the pathophysiology of dyskinesias. There is a long list of etiological factors that can generate dyskinesia; from Huntington disease to perinatal asphyxia itself (Estrada Sánchez et al., 2008) (Montagna et al., 1981). The indirect pathway seems to be involved in the inhibition/filtering of behavior, either at the motor level related to the dorsal striatum and at the emotional-cognitive level, related to the ventral striatum (see (Haber, 2016). Interestingly, it has been reported that levodopa-induced dyskinesia is related to indirect pathway MSN excitotoxicity (Ivanova & Loonen, 2016).

Typical antipsychotic drugs are widely regarded to treat the positive symptoms of schizophrenia by antagonizing dopamine D_2 receptors expressed by striatal MSN of the indirect pathway (Sebel et al., 2017). Antipsychotics act by antagonizing the D2 receptor that is inhibitory, which would generate an increase in the activity of the MSN of the indirect pathway. Our current hypothesis is that asphyxia during birth and antipsychotics act in opposite ways. Asphyxia would decrease the density of MSNs that express the dopamine D2 receptor (inferred from the decrease of calbindin+ neurons by PA), while antipsychotics prevent these neurons from being inhibited by dopamine (see scheme in Figure 7).

4.7 Final considerations:

The factors that contribute to schizophrenia disease are multiple: social, neurodevelopmental and genetic. Each one may contribute to a spectrum of symptoms that eventually reach a certain level of severity that meets the requirements of the diagnosis of schizophrenia. The intention of this work is not to

give a unique explanation of the origin of schizophrenia, we are not even sure that such explanation exists. We propose a mechanism that can explain the generation of vulnerability to schizophrenia produced by PA. In previous works we had seen that deep hypothermia could prevent alterations that mimic negative symptoms of schizophrenia. Now we observed that the same treatment can reverse alterations linked to the positive symptoms or to the dimension of psychosis. Deep hypothermia can be a therapeutic alternative that prevents the deterioration generated by perinatal asphyxia such as dyskinesia and schizophrenia.

Table1: Antibodies used in this study.

Table 2: Statistical information about calbindin and calrretinin cell counts. Coefficient of Error (CE)= standard error of the mean of repeated estimates (frame counts) divided by the mean. The data is shown as percentage.

Table 3: Statistical information about NeuN and DAPI cell counts. Coefficient of Error (CE)= standard error of the mean of repeated estimates (frame counts) divided by the mean. The data is shown as percentage.

Table 4: Statistical information about the anterior commissure results. Coefficient of Error (CE)= standard error of the mean of repeated estimates (frame counts) divided by the mean. The data is shown as percentage.

Table 5: Statistical information about the width of the striatum.

Figure 1: Panoramic NeuN staining of the whole striatum, the red square indicates the sampling zone of the dorsal striatum and the yellow circles indicates the sampling zone of the nucleus accumbens, the white arrow indicates the beginning of the temporal arm of the anterior commissure used as landmark for the posterior end of the structure (a). There was no gross/evident morphological differences in the striatum and the width of the structure was consistent among treated and control groups with no significant differences (unpaired t test P = 0.16) (b). Approximated proportion of the different populations analyzed in this work (c). Dorsal Striatum Bar= 1mm, Nucleus Accumbens Bar= 200µm.

Figure 2. Representative pictures showing calbindin staining of the dorsal striatum (a-d) and nucleus accumbens (NAcc) (f-i). Proportion of neurons among experimental groups compared to VC (100%= 21.2 ± 1,7 cells/0.01 mm^2 in Dorsal Striatum and 15.4 ± 2.2 cells/0.01 mm^2 in NAcc). There was a significant decrease in the relative density of calbindin neurons in the PA group that was prevented by deep hypothermic treatment both in the dorsal striatum (e) and in the NAcc (j). In all cases, deep hypothermia reversed the alterations produced by asphyxia. Bar= 100µm. PA (perinatal asphyxia). CC (caesarean control). HYPPA (hypothermia post asphyxia) VC (vaginal control).

Figure 3 Immunostaining of calretinin and reelin (a, c). PA increases the number of neurons with calretinin in the dorsal striatum and deep hypothermia prevents these alterations. The densities of cells in the control group were in the case of the dorsal

striatum 0.4 ± 0.06 cells / 0.01 mm^2 and 0.44 ± 0.11 cells / mm^2 in the case of ventral striatum. In the dorsal striatum, there was a significant increase of neurons with calretinin produced by asphyxia and the deep hypothermia prevented these alterations (b). In the case of NAcc, a similar pattern was observed but no significant differences were reached. Bar= 50 µm.

Reelin labeling did not show any label in the striatum with the exception of the subventricular zone where there was a group of cells with very strong labeling. Bar=40 µm (Down right).

Figure 4 NeuN immunohistochemistry and DAPI staining. PA produced a significant increase in the number of total neurons of the dorsal striatum estimated by NeuN staining and deep hypothermia prevented this alteration. DAPI stain in the dorsal striatum generated a similar pattern although the differences were not statistically significant. Densities of vaginal control group: 100% = 26.24± 1.65 cells / 0.01 mm^2 for NeuN and 46.35± 5.07cells / 0.01 mm^2 for DAPI. Bar=200 µm. PA (perinatal asphyxia). CC (caesarean control). HYPPA (hypothermia post asphyxia) VC (vaginal control).

Figure 5: NeuN immunohistochemistry and DAPI stain. PA produced a significant increase in the number of total neurons of the nucleus accumbens. Post hoc test between the CC group and the group exposed to asphyxia did not show significant differences. DAPI stain did not reach significant differences. Densities of vaginal control group (100%) were 21.22 ± 1.9 / 0.01 mm^2 for NeuN and 50.89 ± 3.67 /

0.01 mm^2 for DAPI. Bar=200 µm. PA (perinatal asphyxia). CC (caesarean control). HYPPA (hypothermia post asphyxia) VC (vaginal control).

Figure 6: Morphometric analysis of the anterior commissure. DAPI stain of the cells that are inside the anterior commissure showed high consistency. The thickness of the structure in the minor axis showed a notorious and significant shrinkage produced by PA that was reversed by deep hypothermia. The vaginal control values for these parameters were 0.325 ± 0.01 mm in the case of the minor axis of the anterior commissure and 63.83 ± 1.5 / 0.01 mm^2 for DAPI cell counts. Bar=300 µm. PA (perinatal asphyxia). CC (caesarean control). HYPPA (hypothermia post asphyxia) VC (vaginal control).

Figure 7 Graphical abstract; it has been well described that Medium Spiny Neurons comprise more than 95% of striatal neurons. All of them are GABAergic neurons expressing different profiles including calbindin that was reported in Medium Spiny Neurons of the indirect pathway. PA decreases the number of calbindin neurons and increases other neuronal subpopulations. Deep hypothermia prevents these alterations. The present results suggest that therapeutic hypothermia could play an important role in the prevention of neurological and psychiatric pathologies related to alterations of Medium Spiny Neurons such as dyskinesia and psychosis. Green circles represent the neuronal marker NeuN.

References

Alcántara, S., Ruiz, M., D'Arcangelo, G., Ezan, F., De Lecea, L., Curran, T., Sotelo, C., & Soriano, E. (1998). Regional and cellular patterns of reelin mRNA expression in the forebrain of the developing and adult mouse. *Journal of Neuroscience*, *18*(19), 7779–7799. https://doi.org/10.1523/jneurosci.18-19-07779.1998

Anon. (1984). Development of the Rta. In *Shipping World and Shipbuilder* (Vol. 180, Issue 4006). https://doi.org/10.1299/jsmermd.2002.19_3

Arcangeli, S., Tozzi, A., Tantucci, M., Spaccatini, C., De Iure, A., Costa, C., Di Filippo, M., Picconi, B., Giampà, C., Fusco, F. R., Amoroso, S., & Calabresi, P. (2013). Ischemic-LTP in striatal spiny neurons of both direct and indirect pathway requires the activation of D1-like receptors and NO/soluble guanylate cyclase/cGMP transmission. *Journal of Cerebral Blood Flow and Metabolism*, *33*(2), 278–286. https://doi.org/10.1038/jcbfm.2012.167

Ariano, M. A. (1983). Distribution of components of the guanosine 3′,5′-phosphate system in rat caudate-putamen. *Neuroscience*, *10*(3), 707–723. https://doi.org/10.1016/0306-4522(83)90212-9

Arlotta, P., Molyneaux, B. J., Jabaudon, D., Yoshida, Y., & Macklis, J. D. (2008). Ctip2 controls the differentiation of medium spiny neurons and the establishment of the cellular architecture of the striatum. *Journal of Neuroscience*, *28*(3), 622–632. https://doi.org/10.1523/JNEUROSCI.2986-07.2008

Azevedo, F. A. C., Carvalho, L. R. B., Grinberg, L. T., Farfel, J. M., Ferretti, R. E.

L., Leite, R. E. P., Filho, W. J., Lent, R., & Herculano-Houzel, S. (2009). Equal numbers of neuronal and nonneuronal cells make the human brain an isometrically scaled-up primate brain. *Journal of Comparative Neurology*, *513*(5), 532–541. https://doi.org/10.1002/cne.21974

Bakhshi, K., & Chance, S. A. (2015). The neuropathology of schizophrenia: A selective review of past studies and emerging themes in brain structure and cytoarchitecture. *Neuroscience*, *303*, 82–102. https://doi.org/10.1016/j.neuroscience.2015.06.028

Barkhuizen, M., Van de Berg, W. D. J., De Vente, J., Blanco, C. E., Gavilanes, A. W. D., & Steinbusch, H. W. M. (2017). Nitric Oxide Production in the Striatum and Cerebellum of a Rat Model of Preterm Global Perinatal Asphyxia. *Neurotoxicity Research*, *31*(3), 400–409. https://doi.org/10.1007/s12640-017-9700-6

Barkhuizen, M., van den Hove, D. L. A., Vles, J. S. H., Steinbusch, H. W. M., Kramer, B. W., & Gavilanes, A. W. D. (2017). 25 Years of Research on Global Asphyxia in the Immature Rat Brain. *Neuroscience and Biobehavioral Reviews*, *75*, 166–182. https://doi.org/10.1016/j.neubiorev.2017.01.042

Ben-Ari, Y. (2014). The GABA excitatory/inhibitory developmental sequence: A personal journey. *Neuroscience*, *279*, 187–219. https://doi.org/10.1016/j.neuroscience.2014.08.001

Bennett, B. D., & Bolam, J. P. (1993). Two populations of calbindin D28k-immunoreactive neurones in the striatum of the rat. *Brain Research*, *610*(2),

305–310. https://doi.org/10.1016/0006-8993(93)91414-N

Bonestroo, H. J. C., Heijnen, C. J., Groenendaal, F., Van Bel, F., & Nijboer, C. H. (2015). Development of cerebral gray and white matter injury and cerebral inflammation over time after inflammatory perinatal asphyxia. *Developmental Neuroscience*, *37*(1), 78–94. https://doi.org/10.1159/000368770

Brimblecombe, K. R., & Cragg, S. J. (2017). The Striosome and Matrix Compartments of the Striatum: A Path through the Labyrinth from Neurochemistry toward Function. *ACS Chemical Neuroscience*, *8*(2), 235–242. https://doi.org/10.1021/acschemneuro.6b00333

Celio, M. R. (1990). Calbindin D-28k and parvalbumin in the rat nervous system. *Neuroscience*, *35*(2), 375–475. https://doi.org/10.1016/0306-4522(90)90091-H

Chess, P. R., & D'Angio, C. T. (1998). Clonic movements following lorazepam administration in full-term infants. *Archives of Pediatrics & Adolescent Medicine*, *152*(1), 98–99. http://www.ncbi.nlm.nih.gov/pubmed/9452719

Choi, H., Kubicki, M., Whitford, T. J., Alvarado, J. L., Terry, D. P., Niznikiewicz, M., McCarley, R. W., Kwon, J. S., & Shenton, M. E. (2011). Diffusion tensor imaging of anterior commissural fibers in patients with schizophrenia. *Schizophrenia Research*, *130*(1–3), 78–85. https://doi.org/10.1016/j.schres.2011.04.016

Cocas, L. A., Miyoshi, G., Carney, R. S. E., Sousa, V. H., Hirata, T., Jones, K. R., Fishell, G., Huntsman, M. M., & Corbin, J. G. (2009). Emx1-lineage

progenitors differentially contribute to neural diversity in the striatum and amygdala. *Journal of Neuroscience*, *29*(50), 15933–15946. https://doi.org/10.1523/JNEUROSCI.2525-09.2009

Coppen, E. M., & Roos, R. A. C. (2017). Current Pharmacological Approaches to Reduce Chorea in Huntington's Disease. *Drugs*, *77*(1), 29–46. https://doi.org/10.1007/s40265-016-0670-4

DiFiglia, M., Christakos, S., & Aronin, N. (1989). Ultrastructural localization of immunoreactive calbindin-D28k in the rat and monkey basal ganglia, including subcellular distribution with colloidal gold labeling. *Journal of Comparative Neurology*, *279*(4), 653–665. https://doi.org/10.1002/cne.902790411

Drobyshevsky, A. (2017). Concurrent decrease of brain white matter tracts' thicknesses and fractional anisotropy after antenatal hypoxia-ischemia detected with tract-based spatial statistics analysis. *Journal of Magnetic Resonance Imaging*, *45*(3), 829–838. https://doi.org/10.1002/jmri.25407

Estrada Sánchez, A. M., Mejía-Toiber, J., & Massieu, L. (2008). Excitotoxic Neuronal Death and the Pathogenesis of Huntington's Disease. *Archives of Medical Research*, *39*(3), 265–276. https://doi.org/10.1016/j.arcmed.2007.11.011

Fish, I., & Winick, M. (1969). Cellular growth in various regions of the developing rat brain. *Pediatric Research*, *3*(5), 407–412. https://doi.org/10.1203/00006450-196909000-00003

Fleck, T. M., Czerny, M., Hutschala, D., Koinig, H., Wolner, E., & Grabenwoger, M. (2003). The incidence of transient neurologic dysfunction after ascending aortic replacement with circulatory arrest. *Annals of Thoracic Surgery*, *76*(4), 1198–1202. https://doi.org/10.1016/S0003-4975(03)00832-4

Foster-Barber, A., Dickens, B., & Ferriero, D. M. (2001). Human perinatal asphyxia: Correlation of neonatal cytokines with MRI and outcome. *Developmental Neuroscience*, *23*(3), 213–218. https://doi.org/10.1159/000046146

Garas, F. N., Kormann, E., Shah, R. S., Vinciati, F., Smith, Y., Magill, P. J., & Sharott, A. (2018). Structural and molecular heterogeneity of calretinin-expressing interneurons in the rodent and primate striatum. *Journal of Comparative Neurology*, *526*(5), 877–898. https://doi.org/10.1002/cne.24373

George, S., Scotter, J., Dean, J. M., Bennet, L., Waldvogel, H. J., Guan, J., Faull, R. L. M., & Gunn, A. J. (2007). Induced cerebral hypothermia reduces post-hypoxic loss of phenotypic striatal neurons in preterm fetal sheep. *Experimental Neurology*, *203*(1), 137–147. https://doi.org/10.1016/j.expneurol.2006.07.024

Gerfen, C. R., Engber, T. M., Mahan, L. C., Susel, Z., Chase, T. N., Monsma, F. J., & Sibley, D. R. (1990). D1 and D2 dopamine receptor-regulated gene expression of striatonigral and striatopallidal neurons. *Science*, *250*(4986), 1429–1432. https://doi.org/10.1126/science.2147780

Gerfen, C. R., & Scott Young, W. (1988). Distribution of striatonigral and striatopallidal peptidergic neurons in both patch and matrix compartments: an

in situ hybridization histochemistry and fluorescent retrograde tracing study. *Brain Research*, *460*(1), 161–167. https://doi.org/10.1016/0006-8993(88)91217-6

Gerfen, C. R., & Surmeier, D. J. (2011). Modulation of Striatal Projection Systems by Dopamine. *Annual Review of Neuroscience*, *34*(1), 441–466. https://doi.org/10.1146/annurev-neuro-061010-113641

Groenewegen, H. J. (2003). The basal ganglia and motor control. *Neural Plasticity*, *10*(1–2), 107–120. https://doi.org/10.1155/NP.2003.107

Guan, J., Bennet, L., George, S., Waldvogel, H. J., Faull, R. L. M., Gluckman, P. D., Keunen, H., & Gunn, A. J. (1999). Selective neuroprotective effects with insulin-like growth factor-1 in phenotypic striatal neurons following ischemic brain injury in fetal sheep. *Neuroscience*, *95*(3), 831–839. https://doi.org/10.1016/S0306-4522(99)00456-X

Guillery, R. W. (2002). On counting and counting errors. *Journal of Comparative Neurology*, *447*(1), 1–7. https://doi.org/10.1002/cne.10221

Haber, S. N. (2016). Corticostriatal circuitry. *Dialogues in Clinical Neuroscience*, *18*(1), 7–21. https://doi.org/10.1007/978-1-4614-6434-1_135-1

Hennou, S., Khalilov, I., Diabira, D., Ben-Ari, Y., & Gozlan, H. (2002). Early sequential formation of functional GABAA and glutamatergic synapses on CA1 interneurons of the rat foetal hippocampus. *European Journal of Neuroscience*, *16*(2), 197–208. https://doi.org/10.1046/j.1460-

9568.2002.02073.x

Herrera, M. I., Otero-Losada, M., Udovin, L. D., Kusnier, C., Kölliker-Frers, R., De Souza, W., & Capani, F. (2017). Could Perinatal Asphyxia Induce a Synaptopathy? New Highlights from an Experimental Model. *Neural Plasticity*, *2017*, 3436943. https://doi.org/10.1155/2017/3436943

Hurd, Y. L., Suzuki, M., & Sedvall, G. C. (2001). D1 and D2 dopamine receptor mRNA expression in whole hemisphere sections of the human brain. *Journal of Chemical Neuroanatomy*, *22*(1–2), 127–137. https://doi.org/10.1016/S0891-0618(01)00122-3

Ivanova, S. A., & Loonen, A. J. M. (2016). Levodopa-Induced Dyskinesia Is Related to Indirect Pathway Medium Spiny Neuron Excitotoxicity: A Hypothesis Based on an Unexpected Finding. *Parkinson's Disease*, *2016*, 1–5. https://doi.org/10.1155/2016/6461907

Kemp, J. M., & Powell, T. P. (1971). The structure of the caudate nucleus of the cat: light and electron microscopy. *Philosophical Transactions of the Royal Society of London. Series B, Biological Sciences*, *262*(845), 383–401. https://doi.org/10.1098/rstb.1971.0102

Khazipov, R., Esclapez, M., Caillard, O., Bernard, C., Khalilov, I., Tyzio, R., Hirsch, J., Dzhala, V., Berger, B., & Ben-Ari, Y. (2001). Early development of neuronal activity in the primate hippocampus in utero. *Journal of Neuroscience*, *21*(24), 9770–9781. https://doi.org/10.1523/jneurosci.21-24-09770.2001

Kindler, J., Schultze-Lutter, F., Michel, C., Martz-Irngartinger, A., Linder, C., Schmidt, S. J., Stegmayer, K., Schimmelmann, B. G., & Walther, S. (2016). Abnormal involuntary movements are linked to psychosis-risk in children and adolescents: Results of a population-based study. *Schizophrenia Research*, *174*(1–3), 58–64. https://doi.org/10.1016/j.schres.2016.04.032

Koning, J. P., Tenback, D. E., Kahn, R. S., Vollema, M. G., Cahn, W., & Van Harten, P. N. (2011). Movement disorders are associated with schizotypy in unaffected siblings of patients with non-affective psychosis. *Psychological Medicine*, *41*(10), 2141–2147. https://doi.org/10.1017/S0033291711000389

Leaw, B., Nair, S., Lim, R., Thornton, C., Mallard, C., & Hagberg, H. (2017). Mitochondria, bioenergetics and excitotoxicity: New therapeutic targets in perinatal brain injury. *Frontiers in Cellular Neuroscience*, *11*, 199. https://doi.org/10.3389/fncel.2017.00199

Loidl, C. F., De Vente, J., van Ittersum, M. M., van Dijk, E. H., Vles, J. S., Steinbusch, H. W., & Blanco, C. E. (1998). Hypothermia during or after severe perinatal asphyxia prevents increase in cyclic GMP-related nitric oxide levels in the newborn rat striatum. *Brain Research*, *791*(1–2), 303–307. http://www.ncbi.nlm.nih.gov/pubmed/9593957

Loidl, C. F., Herrera-Marschitz, M., Andersson, K., You, Z. B., Goiny, M., O'Connor, W. T., Silveira, R., Rawal, R., Bjelke, B., Chen, Y., & Ungerstedt, U. (1994). Long-term effects of perinatal asphyxia on basal ganglia neurotransmitter systems studied with microdialysis in rat. *Neuroscience*

Letters, *175*(1–2), 9–12. https://doi.org/10.1016/0304-3940(94)91065-0

Mallard, E. C., Waldvogel, H. J., Williams, C. E., Faull, R. L. M., & Gluckman, P. D. (1995). Repeated asphyxia causes loss of striatal projection neurons in the fetal sheep brain. *Neuroscience*, *65*(3), 827–836. https://doi.org/10.1016/0306-4522(94)00504-X

Meloni, B. P., Mastaglia, F. L., & Knuckey, N. W. (2008). Therapeutic applications of hypothermia in cerebral ischaemia. *Therapeutic Advances in Neurological Disorders*, *1*(2), 75–98. https://doi.org/10.1177/1756285608095204

Montagna, P., Cirignotta, F., Gallassi, R., & Sacquegna, T. (1981). Progressive choreo-athetosis related to birth anoxia. *Journal of Neurology, Neurosurgery, and Psychiatry*, *44*(10), 957. https://doi.org/10.1136/jnnp.44.10.957

Morrison, P. D., & Murray, R. M. (2009). From real-world events to psychosis: The emerging neuropharmacology of delusions. *Schizophrenia Bulletin*, *35*(4), 668–674. https://doi.org/10.1093/schbul/sbp049

Ng, E., Klinger, G., Shah, V., Taddio, A., Pérez, A., & Gagnon, L. (2002). Safety of benzodiazepines in newborns. *Annals of Pharmacotherapy*, *36*(7–8), 1150–1155. https://doi.org/10.1345/aph.1A328

Nishikawa, S., Goto, S., Hamasaki, T., Ogawa, M., & Ushio, Y. (1999). Transient and compartmental expression of the reeler gene product Reelin in the developing rat striatum. *Brain Research*, *850*(1–2), 244–248. https://doi.org/10.1016/S0006-8993(99)02136-8

Northington, F. J., Chavez-Valdez, R., & Martin, L. J. (2011). Neuronal cell death in neonatal hypoxia-ischemia. *Annals of Neurology*, *69*(5), 743–758. https://doi.org/10.1002/ana.22419

Ortinau, C. M., Mangin-Heimos, K., Moen, J., Alexopoulos, D., Inder, T. E., Gholipour, A., Shimony, J. S., Eghtesady, P., Schlaggar, B. L., & Smyser, C. D. (2018). Prenatal to postnatal trajectory of brain growth in complex congenital heart disease. *NeuroImage: Clinical*, *20*, 913–922. https://doi.org/10.1016/j.nicl.2018.09.029

Parissis, H., Hamid, U., Soo, A., & Al-Alao, B. (2011). Brief review on systematic hypothermia for the protection of central nervous system during aortic arch surgery: A double-sword tool? *Journal of Cardiothoracic Surgery*, *6*(1), 153. https://doi.org/10.1186/1749-8090-6-153

Paxinos, G., & Watson, C. (2004). *The Rat Brain in Stereotaxic Coordinates - The New Coronal Set*. Academic Press. https://books.google.com/books?id=xzNyLkQ7-q0C&pgis=1

Petryszyn, S., Parent, A., & Parent, M. (2018). The calretinin interneurons of the striatum: comparisons between rodents and primates under normal and pathological conditions. *Journal of Neural Transmission*, *125*(3), 279–290. https://doi.org/10.1007/s00702-017-1687-x

Plum, P. (1965). Aetiology of athetosis with special reference to neonatal asphyxia, idiopathic icterus, and ABO-incompatibility. *Archives of Disease in Childhood*, *40*(212), 376–384. https://doi.org/10.1136/adc.40.212.376

Prensa, L., Giménez-Amaya, J. M., & Parent, A. (1998). Morphological features of neurons containing calcium-binding proteins in the human striatum. *Journal of Comparative Neurology*, *390*(4), 552–563. https://doi.org/10.1002/(sici)1096-9861(19980126)390:4<552::aid-cne7>3.0.co;2-%23

Reynolds, G. P., Abdul-Monim, Z., Neill, J. C., & Zhang, Z. J. (2004). Calcium binding protein markers of GABA deficits in schizophrenia - Post mortem studies and animal models. *Neurotoxicity Research*, *6*(1), 57–61. https://doi.org/10.1007/BF03033297

Robbins, T. W., & Everitt, B. J. (1996). Neurobehavioural mechanisms of reward and motivation. *Current Opinion in Neurobiology*, *6*(2), 228–236. https://doi.org/10.1016/S0959-4388(96)80077-8

Scaravilli, V., Bonacina, D., & Citerio, G. (2012). Rewarming: facts and myths from the systemic perspective. *Critical Care*, *16*(S2), A25. https://doi.org/10.1186/cc11283

Schmitz, C., & Hof, P. R. (2005). Design-based stereology in neuroscience. *Neuroscience*, *130*(4), 813–831. https://doi.org/10.1016/j.neuroscience.2004.08.050

Sebel, L. E., Graves, S. M., Chan, C. S., & Surmeier, D. J. (2017). Haloperidol Selectively Remodels Striatal Indirect Pathway Circuits. *Neuropsychopharmacology*, *42*(4), 963–973. https://doi.org/10.1038/npp.2016.173

Shankaran, S., Woldt, E., Koepke, T., Bedard, M. P., & Nandyal, R. (1991). Acute neonatal morbidity and long-term central nervous system sequelae of perinatal asphyxia in term infants. *Early Human Development*, *25*(2), 135–148. https://doi.org/10.1016/0378-3782(91)90191-5

Sharaf, A., Rahhal, B., Spittau, B., & Roussa, E. (2015). Localization of reelin signaling pathway components in murine midbrain and striatum. *Cell and Tissue Research*, *359*(2), 393–407. https://doi.org/10.1007/s00441-014-2022-6

Simbruner, G., Mittal, R. A., Rohlmann, F., Muche, R., Obladen, Schmitz, T., Muench, G., Flemmer, A., Knuepfer, M., Hanssler, L., Schaible, T., Teig, N., Pohlandt, F., Schloesser, R., Heckmann, M., Ahrens, P., Kirchner, L., Francois, A., Cooper, P. A., … Greisen, G. (2010). Systemic Hypothermia after Neonatal Encephalopathy: Outcomes of neo.nEURO.network RCT. *Pediatrics*, *126*(4), e771-8. https://doi.org/10.1542/peds.2009-2441

Thompson, S. M., Masukawa, L. M., & Prince, D. A. (1985). Temperature dependence of intrinsic membrane properties and synaptic potentials in hippocampal CA1 neurons in vitro. *Journal of Neuroscience*, *5*(3), 817–824. https://doi.org/10.1523/jneurosci.05-03-00817.1985

Tripathi, A., Prensa, L., Cebrían, C., & Mengual, E. (2010). Axonal branching patterns of nucleus accumbens neurons in the rat. *Journal of Comparative Neurology*, *518*(22), 4649–4673. https://doi.org/10.1002/cne.22484

Van De Berg, W. D J, Kwaijtaal, M., De Louw, A. J. A., Lissone, N. P. A., Schmitz,

C., Faull, R. L. M., Blokland, A., Blanco, C. E., & Steinbusch, H. W. M. (2003). Impact of perinatal asphyxia on the GABAergic and locomotor system. *Neuroscience*, *117*(1), 83–96. https://doi.org/10.1016/S0306-4522(02)00787-X

Van De Berg, Wilma D.J., Schmitz, C., Steinbusch, H. W. M., & Blanco, C. E. (2002). Perinatal asphyxia induced neuronal loss by apoptosis in the neonatal rat striatum: A combined TUNEL and stereological study. *Experimental Neurology*, *174*(1), 29–36. https://doi.org/10.1006/exnr.2001.7855

Vázquez-Borsetti, P., Peña, E., Rico, C., Noto, M., Miller, N., Cohon, D., Acosta, J. M., Ibarra, M., & Loidl, F. C. (2016). Perinatal Asphyxia Reduces the Number of Reelin Neurons in the Prelimbic Cortex and Deteriorates Social Interaction in Rats. *Developmental Neuroscience*, *38*(4), 241–250. https://doi.org/10.1159/000448244

Vázquez-Borsetti, P., Peña, E., Rojo, Y., Acuña, A., & Loidl, F. C. (2018). Deep hypothermia reverses behavioral and histological alterations in a rat model of perinatal asphyxia. *Journal of Comparative Neurology*, *July*, 1–10. https://doi.org/10.1002/cne.24539

Watabe-Uchida, M., Zhu, L., Ogawa, S. K., Vamanrao, A., & Uchida, N. (2012). Whole-Brain Mapping of Direct Inputs to Midbrain Dopamine Neurons. *Neuron*, *74*(5), 858–873. https://doi.org/10.1016/j.neuron.2012.03.017

Whitty, P. F., Owoeye, O., & Waddington, J. L. (2009). Neurological signs and involuntary movements in schizophrenia: Intrinsic to and informative on systems pathobiology. *Schizophrenia Bulletin*, *35*(2), 415–424.

https://doi.org/10.1093/schbul/sbn126

Wong, K. C. (1983). Physiology and pharmacology of hypothermia. *Western Journal of Medicine*, *138*(2), 227–232. http://www.ncbi.nlm.nih.gov/pubmed/6837026

Yang, Z., You, Y., & Levison, S. (2008). Neonatal hypoxic/ischemic brain injury induces production of calretinin-expressing interneurons in the striatum. *J Comp Neurol*, *511*(1), 19–33. https://doi.org/10.1002/cne.21819.Neonatal

Zhao, J., Mu, H., Liu, L., Jiang, X., Wu, D., Shi, Y., Leak, R. K., & Ji, X. (2019). Transient selective brain cooling confers neurovascular and functional protection from acute to chronic stages of ischemia/reperfusion brain injury. *Journal of Cerebral Blood Flow and Metabolism*, *39*(7), 1215–1231. https://doi.org/10.1177/0271678X18808174

Zornberg, G. L., Buka, S. L., & Tsuang, M. T. (2000). Hypoxic-ischemia-related fetal/neonatal complications and risk of schizophrenia and other nonaffective psychoses: A 19-year longitudinal study. *American Journal of Psychiatry*, *157*(2), 196–202. https://doi.org/10.1176/appi.ajp.157.2.196

Author contributor statement: PVB: conceived, conducted, performed animal treatments and analyzed the experiments as well as realized contributions to manuscript.LK performed counts, analysis and contributed with the manuscript , AA and MS helped to perform and count the immunohistochemistries, JJL

and CFL contributed with the manuscript.

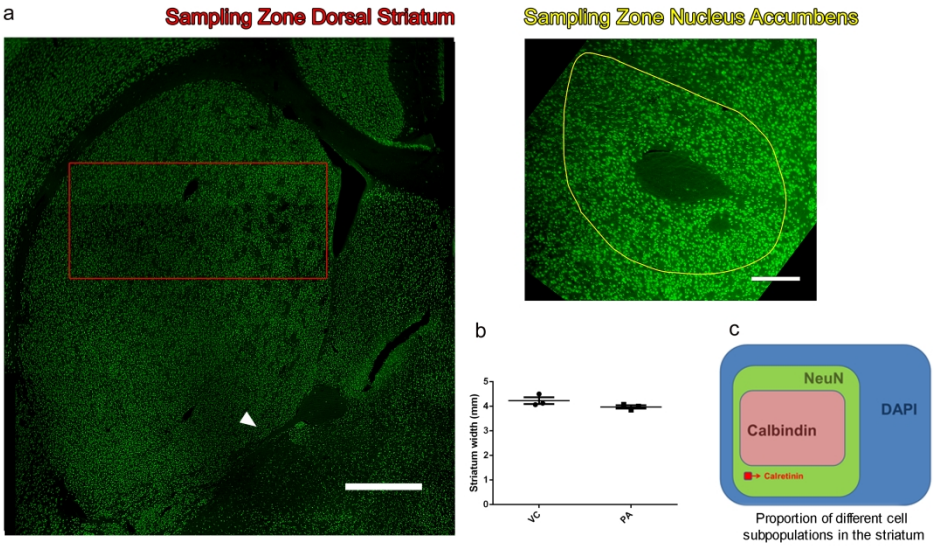

Figure 1: Panoramic NeuN staining of the whole striatum, red square indicates the sampling zone of the dorsal striatum and the yellow circles indicates the sampling zone of the nucleus accumbens, the white arrow indicates the beginning of the temporal arm of the anterior commissure used as landmark for the posterior end of the structure (a). There was no gross/evident morphological differences in the striatum and the width of the structure was consistent among treated and control groups with no significant differences (unpaired t test P = 0.16) (b). Approximated proportion of the different populations analyzed in this work (c). Dorsal Striatum Bar= 1mm, Nucleus Accumbens Bar= 200µm.

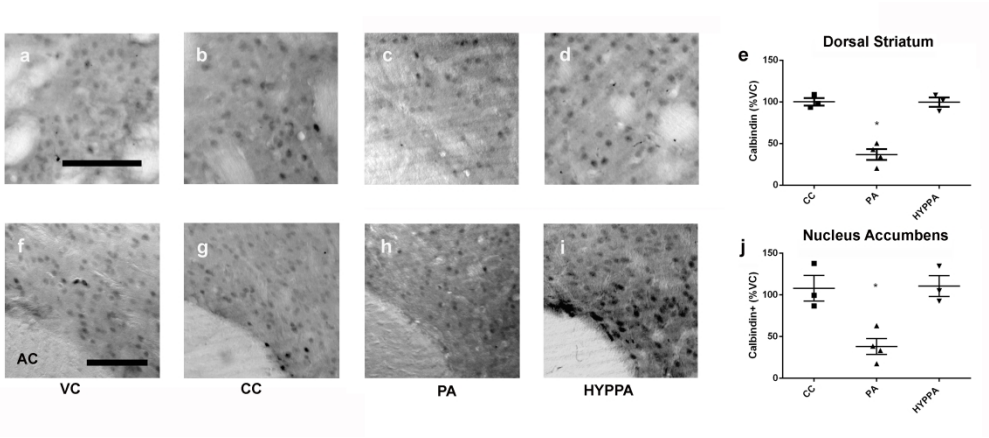

Figure 2. Representative pictures showing calbindin staining of the dorsal striatum (a-d) and nucleus accumbens (NAcc) (f-i). Proportion of neurons among experimental groups compared to VC (100%= 21,2 ± 1,7 cells/0.01 mm2 in Dorsal Striatum and 15,4 ± 2,2 cells/0.01 mm2 in NAcc).). There was a significant decrease in the relative density of calbindin neurons in the PA group that was prevented by deep hypothermic treatment both in the dorsal striatum (e) and in the NAcc (j). In all cases, deep hypothermia reversed the alterations produced by asphyxia. Bar= 100µm. PA (perinatal asphyxia). CC (caesarean control). HYPPA (hypothermia post asphyxia) VC (vaginal control).

331x144mm (300 x 300 DPI)

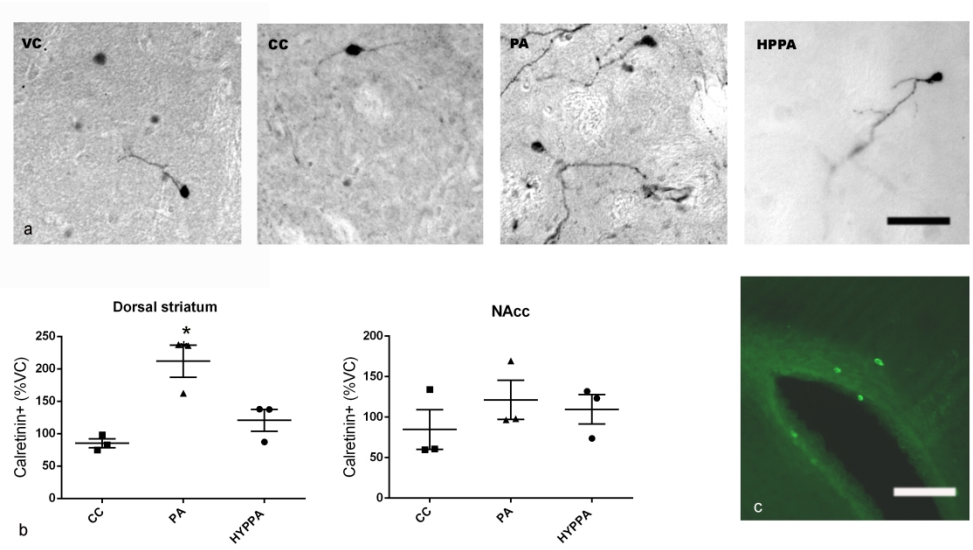

Figure 3 Immunostaining of calretinin and reelin (a, c). PA increases the number of neurons with calretinin in the dorsal striatum and deep hypothermia prevents these alterations. The densities of cells in the control group were in the case of the dorsal striatum 0.4 ± 0,06 cells / 0.01 mm2 and in the case of ventral 0.44 ± 0.11 cells / mm2. In the dorsal striatum, there was a significant increase of neurons with calretinin produced by asphyxia and the deep hypothermia prevented these alterations (b). In the case of NAcc, a similar pattern was observed but no significant differences were reached. Bar= 50 µm.
Reelin labeling did not show any label in the striatum with the exception of the subventricular zone where there was a group of cells with very strong labeling. Bar=40 µm (Down right).

313x174mm (300 x 300 DPI)

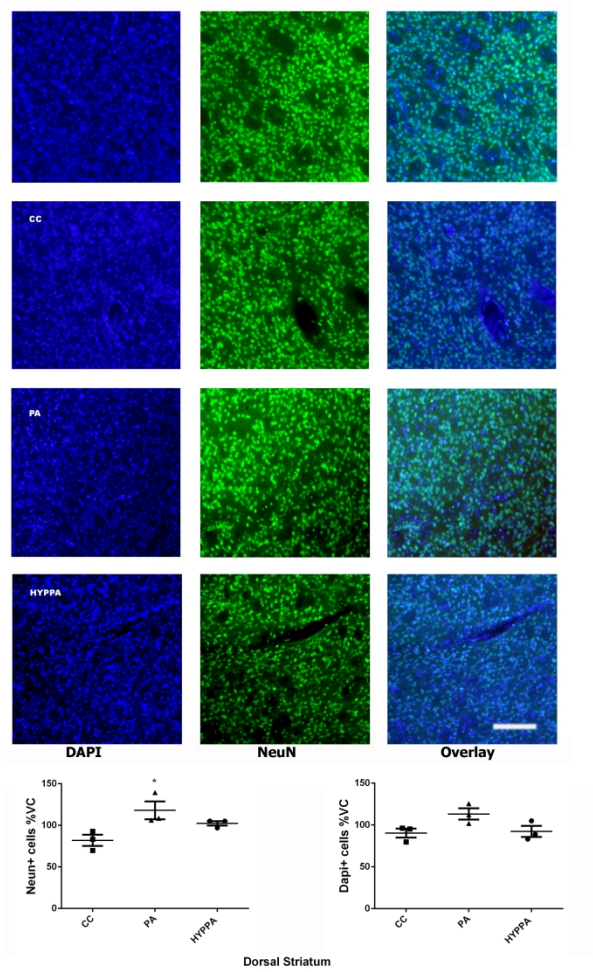

Figure 4 NeuN immunohistochemistry and DAPI staining. PA produced a significant increase in the number of total neurons of the dorsal striatum estimated by NeuN staining and deep hypothermia prevented these alterations. DAPI stain in the dorsal striatum generated a similar pattern although the differences were not statistically significant. Densities of vaginal control group: 100% = 26,24± 1,65 cells / 0.01 mm2 for NeuN and 46,35± 5,07cells / 0.01 mm2 for DAPI. Bar=200 µm. PA (perinatal asphyxia). CC (caesarean control). HYPPA (hypothermia post asphyxia) VC (vaginal control).

299x299mm (300 x 300 DPI)

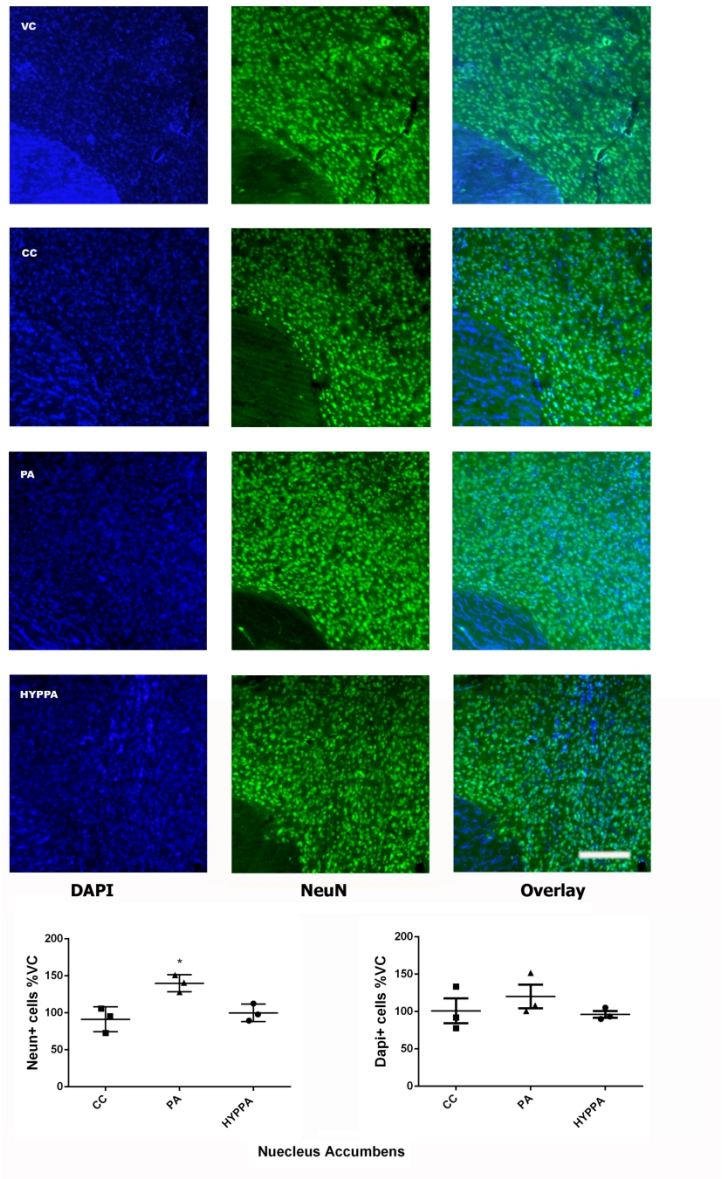

Figure 5: NeuN immunohistochemistry and DAPI stain. PA produced a significant increase in the number of total neurons of the nucleus accumbens. Post hoc test between the CC group and the group exposed to asphyxia did not show significant differences. DAPI stain did not reach significant differences. Densities of vaginal control group (100%) were 21.22 ± 1.9 / 0.01 mm2 for NeuN and 50.89 ± 3.67 / 0.01 mm2 for DAPI. Bar=200 µm. PA (perinatal asphyxia). CC (caesarean control). HYPPA (hypothermia post asphyxia) VC (vaginal control).

180x299mm (300 x 300 DPI)

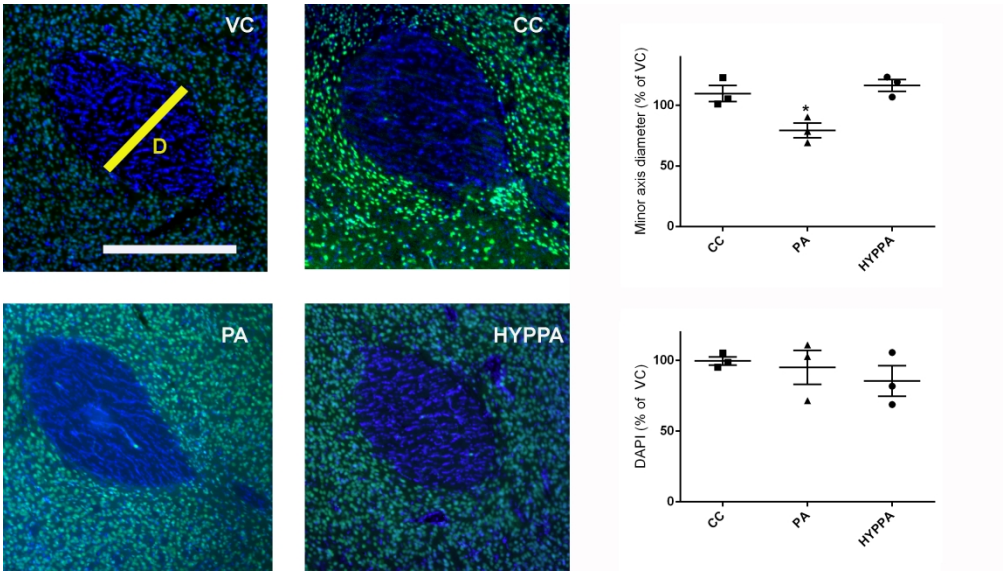

Figure 6: Morphometric analysis of the anterior commissure. DAPI stain of the cells that are inside the anterior commissure showed high consistency. The thickness of the structure in the minor axis showed a notorious and significant shrinkage produced by PA that was reversed by deep hypothermia. The vaginal control values for these parameters were 0.325 ± 0.01 mm in the case of the minor axis of the anterior commissure and 63.83 ± 1.5 / 0.01 mm2 for DAPI cell counts. Bar=300 µm. PA (perinatal asphyxia). CC (caesarean control). HYPPA (hypothermia post asphyxia) VC (vaginal control).

299x169mm (300 x 300 DPI)

Antibody	Antigen	Host	Type	Source	Dilution
Reelin: mouse, human, rat.	Recombinant fusion protein, corresponding to amino acids 164–496 of mouse.	Mouse	Monoclonal	Abcam (ab78540) RRID:AB_1603148	1:1000
Calbindin human, rat.	Prokaryotic recombinant protein corresponding to the majority of the calbindin molecule.	Mouse	Monoclonal	Leica (NCL-CALBINDIN) RRID:AB_563448.	1:1000
NeuN	Purified cell nuclei from mouse brain	Mouse	Monoclonal	Merck Millipore MAB377 clone A60 RRID: AB_2298772	1:1000
Calretinin	Specific for an epitope mapping between amino acids 2-27 at the N-terminus of Calretinin of human origin	Mouse	Monoclonal	Santa Cruz Biotechnology sc-365956 RRID: AB_10846469	1:1000
Secondary antibody	Mouse IGG	Goat	Policlonal Biotinilated	Thermo Fisher Cientific RRID: AB_228305	1:1000
Secondary antibody	Mouse IGG	Goat	Policlonal conjugated with fluorescent alexa	Thermo Fisher Cientific (A32723) RRID: AB_2633275	1:1000

Table1: Antibodies used in this study.

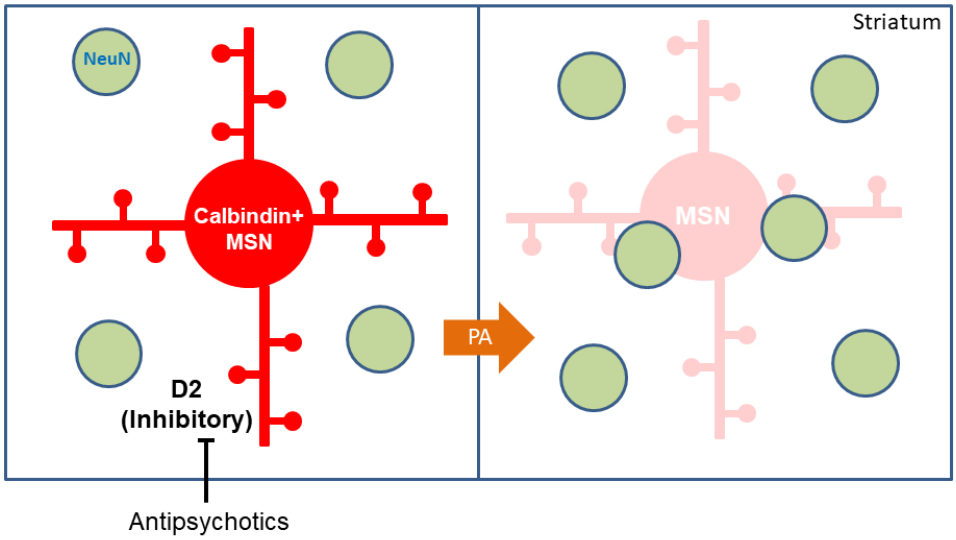

Figure 7: Graphical abstract; it has been well described that Medium Spiny Neurons comprise more than 95% of striatal neurons. All of them are GABAergic neurons expressing different profiles including calbindin that was reported in Medium Spiny Neurons of the indirect pathway. PA decreases the number of calbindin neurons and increases other neuronal subpopulations. Deep hypothermia prevents these alterations. The present results suggest that therapeutic hypothermia could play an important role in the prevention of neurological and psychiatric pathologies related to alterations of Medium Spiny Neurons such as dyskinesia and psychosis. Green circles represent the neuronal marker NeuN.

254x190mm (96 x 96 DPI)

%Calbindin	Dorsal			Ventral		
	CE(VC)= 6,80%			CE(VC)= 6,41%		
	CC	PA	HYPPA	CC	PA	HYPPA
Number of values	3	4	3	3	4	3
Minimum	93,67	20,28	88,99	86,7	17,39	92,54
Median	98,04	38,39	101,8	99,39	35,93	104,9
Maximum	108,8	50,37	108,2	137,8	63,02	134,5
Mean	100,2	36,86	99,66	108	38,07	110,7
Std. Deviation	7,791	12,93	9,78	26,62	18,91	21,57
Std. Error of Mean	4,498	6,464	5,646	15,37	9,457	12,46
Lower 95% CI of mean	80,82	16,29	75,37	41,84	7,972	57,06
Upper 95% CI of mean	119,5	57,43	124	174,1	68,17	164,2
Coefficient of variation	7,78%	35,07 %	9,81%	24,66%	49,68 %	19,50%
%Calretinin	Dorsal			Ventral		
	CE(VC)= 13,10%			CE(VC)= 13,36%		
	CC	PA	HYPPA	CC	PA	HYPPA
Number of values	3	3	3	3	3	3
Minimum	74,64	162,3	87,09	59,8	96,56	73,81
Median	82,87	236	137,4	60,5	98,05	123,2
Maximum	98,27	237,4	137,9	133,9	169,4	131,9
Mean	85,26	211,9	120,8	84,73	121,3	109,6
Std. Deviation	12	42,95	29,18	42,58	41,62	31,34
Std. Error of Mean	6,926	24,8	16,85	24,58	24,03	18,09
Lower 95% CI of mean	48,29	55,46	105,2	31,8	-21,04	17,94
Upper 95% CI of mean	193,3	115,1	318,6	187,5	190,5	224,7
Coefficient of variation	24,16%	14,07	20,27%	28,58%	50,25	34,30%

		%			%	

%NeuN	Dorsal			Ventral		
	CE(VC)= 6,80%			CE(VC)= 6,80%		
	CC	PA	HYPPA	CC	PA	HYPPA
Number of values	3	3	3	3	3	3
Minimum	69,67	106,1	96,97	72,73	128	89,47
Median	83,33	108,6	105,1	95,23	140,7	97,89
Maximum	92,85	139,4	105,1	105,8	151,1	112,6
Mean	81,95	118	102,4	91,26	139,9	100
Std. Deviation	11,65	18,54	4,699	16,9	11,55	11,72
Std. Error of Mean	6,728	10,7	2,713	9,755	6,671	6,768
Lower 95% CI of mean	53	71,99	90,72	49,29	111,2	70,88
Upper 95% CI of mean	110,9	164,1	114,1	133,2	168,6	129,1
Coefficient of variation	14,22 %	15,70 %	4,59%	18,51 %	8,26%	11,72 %
%DAPI	dorsal			ventral		
	CE(VC)=6,09%			CE(VC)= 4.71%		
	CC	PA	HYPPA	CC	PA	HYPPA
Number of values	3	3	3	3	3	3
Minimum	79,7	101,9	83,21	77,63	100,5	90
Median	95,3	112,1	88,89	91,89	108,2	93,42
Maximum	96,36	125,5	105	133,3	151,8	105,2
Mean	90,45	113,2	92,37	101	120,2	96,22
Std. Deviation	9,332	11,83	11,3	28,94	27,61	7,989
Std. Error of Mean	5,388	6,833	6,527	16,71	15,94	4,612
Lower 95% CI of mean	67,27	83,81	64,28	29,07	51,58	76,37
Upper 95% CI of mean	113,6	142,6	120,4	172,8	188,8	116,1
Coefficient of variation	10,32 %	10,45 %	12,24 %	28,66 %	22,98 %	8,30%

% of DAPI stained nucleus inside the anterior commissure.			
	CC	PA	HYPPA
Number of values	3	3	3
Minimum	95,22	71,52	68,89
Median	98,57	102,9	81,84
Maximum	105,1	111	105,7
Mean	99,63	95,12	85,46
Std. Deviation	5,023	20,84	18,64
Std. Error of Mean	2,9	12,03	10,76
Lower 95% CI of mean	87,16	43,37	39,15
Upper 95% CI of mean	112,1	146,9	131,8
Coefficient of variation	5,04%	21,90%	21,82%
Length of the minor axis of the anterior commissure.			
	CC	PA	HYPPA
Number of values	3	3	3
Minimum	101,1	69,23	106,8
Median	105,4	78,62	119,2
Maximum	122,8	90,31	123,2
Mean	109,7	79,38	116,4
Std. Deviation	11,48	10,56	8,586
Std. Error of Mean	6,63	6,097	4,957
Lower 95% CI of mean	81,22	53,15	95,08
Upper 95% CI of mean	138,3	105,6	137,7
Coefficient of variation	10,46%	13,30%	7,38%

Width of the striatum		
	VC	PA
Number of values	3	3
Minimum	4,067	3,850
Median	4,125	4,000
Maximum	4,500	4,075
Mean	4,231	3,975
Std. Deviation	0,2350	0,1146
Std. Error of Mean	0,1357	0,06614
Lower 95% CI of mean	3,647	3,690
Upper 95% CI of mean	4,815	4,260
Coefficient of variation	5,56%	2,88%